

1 **COMPARATIVE ADSORPTION OF TETRACYCLINES ON BIOCHARS**
2 **AND STEVENSITE: LOOKING FOR THE MOST EFFECTIVE**
3 **ADSORBENT**

4 Rafael Antón-Herrero^a, Carlos García-Delgado^{a,c*}, María Alonso-Izquierdo^a, Gabriel
5 García-Rodríguez^a, Jaime Cuevas^b, Enrique Eymar^a.

6 ^a*Department of Agricultural Chemistry and Food Sciences, Autonomous University of*
7 *Madrid, 28049 Madrid, Spain.*

8 ^b*Department of Geology and Geochemistry, Autonomous University of Madrid, 28049*
9 *Madrid, Spain.*

10 ^c*Institute of Natural Resources and Agrobiology of Salamanca (IRNASA-CSIC), Cordel*
11 *de Merinas 40-52, 37008 Salamanca, Spain.*

12 ***Corresponding author:**

13 Carlos García-Delgado.
14 Department of Agricultural Chemistry and Food Sciences, Autonomous University of
15 Madrid, Madrid, 28049, Spain.

16 E-mail: carlos.garciadelgado@uam.es

17 Phone: +0034914975010 Fax: +0034914973826

18 **Present address:**

19 Carlos García-Delgado: Institute of Natural Resources and Agrobiology of Salamanca
20 (IRNASA-CSIC), Cordel de Merinas 40-52, 37008 Salamanca, Spain.

21 E-mail: carlos.garcia@irnasa.csic.es

22

23 **E-mail address of each author:**

24 Antón-Herrero, Rafael: rafael.anton@estudiante.uam.es

25 García-Delgado, Carlos: carlos.garciadelgado@uam.es; carlos.garcia@irnasa.csic.es

26 Alonso-Izquierdo, María: maria.alonsoi@estudiante.uam.es

27 García-Rodríguez, Gabriel: gabriel.garcia@estudiante.uam.es

28 Cuevas, Jaime: jaime.cuevas@uam.es

29 Eymar, Enrique: enrique.eymar@uam.es

30 **Abstract**

31 Tetracyclines are one of the most widely used class of veterinary and human antibiotics.
32 The conventional treatment of wastewater based on activated sludge is not effective to
33 remove antibiotics and their residues are still biologically active, which represents a
34 problem in terms of bacterial resistance.

35 The main objective of this work is to assess ability of stevensite and two biochars to
36 adsorb three tetracycline antibiotics from water. Batch adsorption experiments were
37 carried out to test the ability of these materials to adsorb tetracyclines. Then desorption
38 experiments were performed to determine the adsorption strength on stevensite. In order
39 to elucidate the adsorption mechanism of tetracyclines on stevensite, cation exchange
40 analysis and spectroscopic analyses by IR and XRD were performed. The adsorption of
41 tetracyclines on stevensite was tested on continuous system with water artificially
42 contaminated. Finally, the designed filter was validated with tetracyclines spiked
43 wastewater.

44 The two biochars and stevensite were able to adsorb between 60 and 100% of the
45 tetracyclines present in the batch system. Stevensite was the material with the highest
46 tetracyclines removal capacity (around 100% at low concentrations of tetracyclines).
47 Biochars showed less affinity for tetracyclines adsorption (70%). Tetracyclines
48 desorption from stevensite reached values lower than 10% for low tetracyclines
49 concentrations. The IR spectroscopy suggested that cation exchange is the main
50 mechanism of tetracyclines adsorption on clay and also proved the role of amide and
51 amine groups in this adsorption. The cation exchange mechanism was confirmed by
52 displacement of Ca and Mg from stevensite. A continuous wastewater flow through a
53 system composed by stevensite leaved this system with no tetracyclines, indicating
54 water purification by tetracyclines adsorption in clay.

55 **Keywords:** Antibiotics, Clay, Wastewater, Desorption, Water pollution, Continuous
56 System.

57 **1. Introduction**

58 The presence of drugs in the environment is largely due to its incomplete disposal in
59 wastewater treatment plants (WWTP) (Cruz-Morató et al., 2013). Because sewage
60 treatment plants are not adequately equipped to eliminate these substances completely,
61 some are discharged directly into rivers (Valcárcel et al., 2011), through the effluent and
62 dewatered sludge (Hou et al., 2016); which means a contamination of the environment
63 and water sources as well as aquaculture-produced food products (Akinbowale et al.,
64 2016). Because wastewater treatment is only partially effective in removing
65 pharmaceutically active compounds (Pal et al., 2013), abundant studies detected
66 residues of antibiotics in surface and ground water samples around the world
67 (Gavrilescu et al., 2015; López-Serna et al., 2013; Meffe and de Bustamante, 2014;
68 Meritxell et al., 2007; Osorio et al., 2012). Tetracyclines (TCs), including
69 oxytetracycline (OTC), tetracycline (TC) and chlortetracycline (CTC), are some of the
70 most commonly used antibiotics in animal husbandry. In the year 2013, 2957 t of
71 tetracyclines were sold for veterinary therapy only in Europe (Agency, 2013). Generally
72 between 50-80% of a given dose is excreted via the urine as the original compound,
73 although several factors may influence renal elimination, including age, route of
74 administration, urine pH, glomerular filtration rate, and the type of tetracycline used
75 (Halling-Sorensen et al., 2002). The low metabolization rate of antibiotics causes its
76 presence in wastewater (Gros et al., 2007). Concentrations range of antibiotics from ng
77 L⁻¹ to µg L⁻¹ are typical in domestic wastewater but up to 500 mg L⁻¹ have been detected
78 in effluents from farms, hospitals and pharmaceutical industries wastewater (Jing et al.,
79 2014). So, the antibiotics input in wastewater linked with the low efficiency of WWTP

80 to remove pharmaceutical compounds generates antibiotic resistant bacteria and genes
81 in wastewater and they contribute to the discharge of antibiotic resistant bacteria and
82 genes into the environment (Berendonk et al., 2015). TCs resistance is common in
83 bacterial species (Kümmerer, 2009). The frequency of this resistance depends on the use
84 of TCs in human and animals (Andersen and Sandaa, 1994). Kim et al. (2007) showed
85 that increased influent TC concentrations generally increased the concentration,
86 production and percentages of TC intermediate and resistant bacteria under typical
87 activated sludge operating conditions. Therefore, it is important to prevent the
88 antibiotics dissemination into the environment.

89 Among the techniques that exist to remove antibiotics, stand out biodegradation,
90 chemical oxidation, photocatalytic degradation and photoelectrocatalytic degradation.
91 One of the ways of removing TCs or other pharmaceutical compounds is adsorption on
92 clays, such as smectites (Mohd Amin et al., 2016; Wu et al., 2016). However, there is
93 still a growing demand for the development of effective and cost-effective treatments
94 for the elimination of these drugs (Chang et al., 2014).

95 One of the ways of removing TCs or other pharmaceutical compounds is adsorption on
96 clays, biochar, activated carbon, iron and manganese oxides or ion exchange resins
97 (Ahmed et al., 2015; Jiang et al., 2015; Liu et al., 2017; Mohd Amin et al., 2016; Wu et
98 al., 2016; Zhao et al., 2014). Table 1 shows a relation of TCs adsorption capacity of
99 various materials. The chemical speciation of TCs based on the pH of the solution is
100 very important for the adsorption process. TCs are amphoteric chemicals with three
101 ionizable functional groups: dimethylamino group (pK_a 3.3), phenolic diketone group
102 (pK_a 7.3 -7.7) and tricarbonylamide group (pK_a 9.1 -9.7) (Fig 1). The different TCs
103 species in solution are the cationic form (TCH_3^+) at $pH < 3.3$, zwitterionic form (TCH_2)

104 at $3.3 < \text{pH} < 7.7$, monovalent anion (TCH^-) at $7.7 < \text{pH} < 9.7$ and divalent anion (TC^{2-})
105 at $\text{pH} > 9.7$.

106 One of the most promising ways of removing TCs is adsorption on clays, such as
107 smectites (Wu et al., 2016). Smectite clay minerals are used in a wide range of industrial
108 applications, from absorbents to drilling fluids and nano-composites (Bailey et al.,
109 2014). The interaction between TC and clays such as montmorillonite, hectorite,
110 attapulgite or kaolinite, was related to the surface charge of the clay particles (Browne
111 et al., 1980). The main mechanism of adsorption of TC was cation exchange for
112 smectites although the possibility for another adsorption mechanism such as hydrogen
113 bonding or hydrophobic interactions were described by Parolo et al. (2008). The
114 chemical speciation of TCs, whose is controlled by the pH of the solution, is a key
115 factor that determines the affinity of this adsorbent towards TCs. In this respect Parolo
116 et al. (2008) reported that the adsorption constants of the different TC species decrease
117 in the order TCH_3^+ , TCH_2 and TCH^- . And the optimum adsorption pH range is 2 - 4 that
118 corresponds with the TCH_3^+ specie. Other works reported the positive role of the
119 multivalent cations in the TCs adsorption by smectites due to the bridge effect of
120 divalent cations and enhancement of the interlayer trapping of TCs (Aristilde et al.,
121 2016a; Zhao et al., 2012). Biochar is a porous carbonaceous material produced through
122 pyrolysis of biomass that contains numerous oxygen functional groups and aromatic
123 surfaces. The type and concentration of surface functional groups play important roles
124 in the adsorption capacity of the biochar, and in explaining the adsorbate removal
125 mechanism (Qambrani et al., 2017). This material can be produced from lignocellulosic
126 biomass in large scale and at low-cost (Yao et al., 2011). Biochar is effective to adsorb
127 contaminants such as metals and organic pollutants including pesticides, polycyclic
128 aromatic hydrocarbons or veterinary antibiotics (Srinivasan et al., 2015). And the

129 employment of biochar for the removal of organic and heavy metal contaminants from
130 aqueous media is a relatively new and promising water and wastewater treatment
131 technology (Qambrani et al., 2017). It can be used as adequate adsorbent for no-
132 biodegradable organic pollutants before or after the biodegradation process in WWTPs.
133 Previous works on TC adsorption indicate that the alkali biochar possesses an excellent
134 adsorption capacity (58.8 mg g^{-1}), attributed to its large specific surface area and porous
135 structure. The graphite-like structure of alkali biochar facilitates the formation of $\pi - \pi$
136 interactions between ring structure of TC molecule and graphite-like sheets (Liu et al.,
137 2012a).

138 The goals of this work were: i) to select the most adequate adsorbent of TCs between
139 two biochars and stevensite clay, ii) to determine desorption of TCs from the selected
140 material, iii) to elucidate the main mechanism of TCs adsorption and iv) to design a
141 filter able to remove TCs from wastewater in continuous flow.

142 **2. Materials and methods**

143 **2.1. Materials and chemicals**

144 Three materials were tested for TCs adsorption, the clay stevensite and two biochars.
145 The clay used for this study is a raw stevensite (richness > 90%) supplied by Tolsa S.A.
146 (Spain) with the commercial name of Minclear N100. Table 2 summarizes the most
147 important characteristics of stevensite (Mohd Amin et al., 2016; González-Santamaría et
148 al., 2017). Two commercial biochars supplied by Piroeco Bioenergy SL (Spain) were
149 tested. The first one was holm oak pruning (Biochar HO) pyrolyzed at $500 \text{ }^\circ\text{C}$ with
150 particle size less than 8 mm. The second one was a mixture of oak, eucalyptus and pine
151 pruning's (Biochar M) pyrolyzed at $900 \text{ }^\circ\text{C}$ whose granulometry was less than 2 mm (of
152 which 50% was less than 0.5 mm). The characteristic of both biochars are shown in
153 Table 3.

154 Oxytetracycline hydrochloride (OTC, 95% purity), tetracycline hydrochloride (TC, 95%
155 purity) and chlortetracycline hydrochloride (CTC, 97% purity) (Fig. 1) were obtained
156 from Sigma-Aldrich (Spain). Sodium nitrate, nitric acid and sodium hydroxide of
157 analytical grade and acetonitrile and methanol of HPLC grade were provided by
158 Panreac (Spain). Type I deionized water (resistivity = $18.2 \text{ M}\Omega \text{ cm}^{-1}$) was used
159 throughout this study.

160 **2.2. Adsorption isotherms of TCs in stevensite and biochars**

161 Adsorption isotherms were performed with initial TCs (OTC, TC and CTC)
162 concentrations of 50, 100, 200, 300, 400, 500, 600, 800 and 1000 mg L^{-1} for stevensite
163 and biochars HO and M. The solutions of TCs were made in 0.01 M NaNO_3 in order to
164 maintain the ionic strength of the medium and the pH was adjusted in all cases to 2.0
165 with HNO_3 . Twenty mL of each solution were added to 50 mL centrifuge tubes
166 containing 100 mg of stevensite or biochar. The assay was performed in triplicate and a
167 control without adsorbent was placed for each concentration. TCs solutions were
168 prepared just prior to use because they are long-term unstable in the aqueous medium
169 (Kühne et al., 2000). The suspensions were purged with nitrogen in order to displace the
170 oxygen to prevent possible oxygen-mediated degradation of TCs (Zhao et al., 2012).
171 The suspensions were stirred for 24 h at $25 \text{ }^\circ\text{C}$ and 200 rpm on a thermostatic swing-
172 over stirrer in darkness to prevent exposure to light. The interaction was performed per
173 triplicate.

174 After the interaction, the pH of each suspension was measured and then centrifuged
175 (10000 rpm , 10 min). The supernatant was filtered through a $0.45 \text{ }\mu\text{m}$ syringe filter and
176 analyzed by HPLC-PDA. The data obtained were fitted to Langmuir and Freundlich
177 models according to the follow equations:

178 Langmuir model: $Q_e = \frac{Q_{max}a_L C_e}{1+(a_L C_e)}$

179 Freundlich model: $Q_e = K_f C_e^{1/n}$

180 Where Q_e is the amount of TCs adsorbed on solid at equilibrium (mg g^{-1}), C_e is the
181 equilibrium TCs concentration (mg L^{-1}), Q_{max} is the maximum adsorption capacity (mg
182 g^{-1}), a_L is the Langmuir constant, K_f is the Freundlich constant and n is the Freundlich
183 exponent.

184 **2.3. Desorption of immobilized TCs**

185 Desorption experiments with solution of NaNO_3 0.01 M at pH 2 and 7.5 were
186 performed sequentially after adsorption isotherm, under the same conditions used in
187 adsorption experiments (200 rpm, 24 h, 25 °C, darkness, N_2 atmosphere).

188 **2.4. Spectrometric analysis**

189 The solid residue obtained after isothermal adsorption of TCs on stevensite at initial
190 concentration of 1000 mg L^{-1} were freeze dried. Original hydrochloride of TCs and
191 stevensite after TCs isotherm adsorption were subjected to Kubelka-Munk transformed
192 infrared spectroscopy (KMT-IR) using a Bruker IFS66v spectrometer (Billerica, MA,
193 USA); readings were obtained in arbitrary units of diffuse reflectance. Samples (2 mg)
194 were diluted in 98 mg of KBr previous analysis. Spectra were obtained by accumulating
195 250 scans at a resolution of 4 cm^{-1} .

196 **2.5. Adsorption of TCs in continuous flow**

197 Adsorption on continuous system was performed per triplicate in pressurized glass
198 columns (GE Healthcare Column ASSY XK50/30) of 50 mm of internal diameter. The
199 columns were filled with 10 g of stevensite mixed with 90 g of milled glass in order to
200 prevent compaction. Firstly, the filter was evaluated with artificial effluent whose

201 composition was OTC, TC and CTC at 50 mg L⁻¹ in NaNO₃ 0.05 M at pH 7.0.
202 Secondly, the filter was validated with wastewater collected from the wastewater
203 treatment plant of the Autonomous University of Madrid. The pH and electrical
204 conductivity were 7.48 and 555 μS cm⁻¹, respectively. Wastewater was spiked with
205 OTC, TC and CTC at 50 mg L⁻¹ immediately previous to the assay. Samples of the
206 effluent after filtration through stevensite were collected at regular intervals for
207 determination of residual concentration of TCs by HPLC-PDA.

208 **2.6. Analysis of TCs by HPLC-PDA**

209 HPLC analysis were performed using a system composed of a separation module (2695
210 Waters, Milford, MA) equipped with an Agilent ZORBAX SB-C8 separation column
211 (250 × 4.6 mm, 5 micron particle size) and photodiode array detector (Waters 996
212 PDA). Chromatographic separation of TCs was achieved by a linear gradient elution
213 program using (A) 10 mM trifluoroacetic acid (TFA), (B) acetonitrile and (C) methanol
214 at flow rate of 1.5 mL min⁻¹. The elution program is resumed in Table 4. The
215 temperature of the column was set at 28° C. The sample injection volume was 20 μL.
216 Chromatograms were monitored and quantified at 355 nm. TCs were identified using
217 both their UV spectra (200-400 nm) and retention times based on commercially
218 available standards (Sigma-Aldrich).

219 **2.7. Statistical methods used**

220 For the fitting of the isotherms the Solver plug-in of the program Microsoft Excel was
221 used. Data were statistically evaluated by one-way ANOVA followed by Duncan post-
222 hoc test ($p \leq 0.05$) using the software IBM SPSS Statistics v20.

223 3. Results and discussion

224 3.1. Adsorption isotherms of TCs on stevensite and biochars

225 The initial pH of the TCs solutions was adjusted to 2 but after 24 h of interaction with
226 the adsorbents, the pH of the suspensions increased to a range of 3.80 to 5.19 for
227 stevensite, 2.51 to 6.29 for biochar HO and 2.16 to 6.43 for biochar M. The increment
228 of pH was function of the type of tetracycline, initial concentration of antibiotic and the
229 buffer capacity of the adsorbent. At higher initial TCs concentrations, lower pH were
230 measure because the acid nature of these antibiotics. Respect to the nature of the
231 antibiotics, CTC showed higher pH values than OTC and finally TC. The buffer
232 capacity of the adsorbents was caused by the basic nature of stevensite (Khoury et al.,
233 1982; Mohd Amin et al., 2016), HO and M biochar with pH values of 8.44, 9.29 and
234 9.73 respectively (Tables 2 and 3). The basic nature of stevensite is related with itself
235 natural origin that is linked to alkaline aqueous media precipitation in saline-alkaline
236 lakes at $\text{pH} > 9$ (Khoury et al., 1982). The high pH values of biochar are because of the
237 formation of carbonates during the pyrolysis process.

238 According to the pKa values of the TCs (Fig. 1), at the pH range at the end of the
239 interaction with stevensite (3.80 to 5.19) the major ionic form was the specie TCH_2^\pm due
240 to the loss of a proton from the phenolic diketone fraction and the protonation of the
241 dimethyl-ammonium group (Fig. 2). Therefore the zwitterionic TCH_2^\pm was the specie
242 adsorbed on stevensite. In contrast, in biochar adsorption isotherms, two species were
243 the major forms, TCH_3^+ at pH close to 2 and the zwitterionic form TCH_2^\pm at pH over
244 3.3.

245 Isotherms of TCs adsorption on the three materials are showed in Fig. 3 and the
246 adsorption parameters of Freunlich and Langmuir models are in Table 5. The quadratic
247 correlation values indicate the good adjustment of the points to the two isotherm

248 models. The n parameter of the Freundlich model was greater than 1, which means that
249 the adsorption was favorable. The stevensite values of Freundlich constant (K_f) were
250 higher than biochars indicating higher TCs adsorption by stevensite than biochar HO
251 and M. This trend was confirmed by the highest values of maximum adsorption
252 capacity (Q_m) of Langmuir model for stevensite. The values of Q_m indicated that
253 stevensite showed high adsorption capacity of TCs, 126, 127 and 140 mg g^{-1} of OTC,
254 TC and CTC respectively (Table 5).

255 This adsorption increases until a maximum (Q_{max}) is reached, which could be explained
256 by the effect of the cation exchange (Jiang et al., 2015). If this is the mechanism by
257 which the TCs are adsorbed in the stevensite, there will be a point where no more
258 negatively charged sites remain in the clay and a saturation state is reached where
259 tetracycline is no longer adsorbed (Chang et al., 2014). This adsorption could be
260 possible due to the antibiotic's bound to the clay by electrostatic forces between the
261 positively charged TCs and the negative charge of the clay as well as it is housed in the
262 interlaminar space of the clay (Chang et al., 2009a).

263 The results of the biochar isotherms (Fig. 3b and 3c) showed a better fit to the Langmuir
264 model (Table 5). The maximum adsorption capacities of biochar HO were 44, 12 and 18
265 mg g^{-1} for OTC, TC and CTC respectively and in the case of biochar M the Q_m values
266 were 25, 15 and 18 mg g^{-1} of OTC, TC and CTC respectively (Table 5). Comparing the
267 results of biochars isotherms we concluded that both biochars had reached the saturation
268 according to the Langmuir fit for TC. In the case of OTC, saturation has been reached in
269 biochar M, but the biochar HO still continues to exhibit adsorption capacity for OTC.

270 The same trend was observed for CTC, meaning that the biochar HO had a better
271 adsorption capacity for TCs. The adsorption of TCs in biochar was produced through
272 hydrogen bonds through the functional groups of the biochar such as $-\text{OH}$ or $-\text{COOH}$

273 (Liu et al., 2012b). Tan et al., (2015) exposed that the higher the pyrolysis temperature
274 to which it is subjected, the higher the adsorption capacity the material is due to the
275 higher carbonization of the organic matter (higher percentage of C). However in this
276 case, the higher adsorption capacity of biochar OH than M could be related with the
277 higher specific surface of biochar OH (Table 3).

278 Different values of Q_{\max} of previous published works using different supports are shown
279 in Table 1. For different montmorillonite clays the Q_{\max} had values between 125 and
280 192 mg g^{-1} (Chang et al., 2014). However the Q_{\max} of clays was strongly influenced by
281 pH (Chang et al., 2014) and the background solution used for the interaction, in this
282 respect montmorillonite with intercalated iron particles showed a Q_{\max} value of 316.5
283 mg g^{-1} in a 0.1 mol L^{-1} NaCl solution, 339.0 mg g^{-1} using a 0.1 mol L^{-1} solution of
284 NaNO_3 and 689.9 mg g^{-1} using a 0.1 mol L^{-1} solution of NaH_2PO_4 (Wu et al., 2016). In
285 comparison, the Q_{\max} of the stevensite was higher than the biochars HO and M. The
286 adsorption capacity of stevensite is promising compared with others materials of Table
287 1. Therefore, stevensite was used to design a continuous system to test the stevensite
288 ability to uptake TCs from wastewater in continuous flow.

289 **3.2. Desorption of immobilized TCs in stevensite**

290 The TCs desorption (Fig. 4) is more influenced by the concentration of TCs adsorbed
291 than the pH of the solution. At low TCs concentration the desorption process was low or
292 negligible because re-adsorption phenomena on stevensite. The most susceptible TCs
293 for desorption was OTC followed by TC and finally CTC. CTC was the most adsorbed
294 antibiotic followed by TC and finally OTC. Therefore desorption behaviour agreed the
295 stevensite affinity to the different TCs. Concentrations of OTC, TC and CTC below 80,
296 100 and 120 mg g^{-1} , respectively, reported desorption percentages lower than 10% at pH
297 2. These results are in agreement with Jiang et al. (2015), who suggested the high

298 resistance of TC to be desorbed from birnessite. Additionally, Yao et al., (2016)
299 observed that desorption of OTC in soil organic matter did not significantly varied
300 between pH 2 to 6 at low concentrations.

301 At pH 2, TCs desorption reached the maximum value when the initial concentration was
302 the highest studied being 19% for TC at 105 mg g⁻¹, 23% for OTC at 99 mg g⁻¹ and 14 %
303 for CTC at 126 mg g⁻¹. Desorption lower than 1% was observed in the smallest
304 concentration ranges 9-38 mg g⁻¹ for TC, 9-36 mg g⁻¹ for OTC and 9-55 mg g⁻¹ for CTC.

305 At pH 7, OTC desorption was 4% for 9 mg g⁻¹ and 10% between 69-89 mg g⁻¹. The
306 maximum desorption of TC at pH 7 was 8% which corresponds to the highest amount
307 of TC adsorbed (97 mg g⁻¹). CTC desorption was lower than 3% for all the
308 concentrations at pH 7. The desorption preference OTC > TC > CTC was in agreement
309 with the higher CTC values of Freundlich's and Langmuir's constants (K , a_L and Q_{max} ,
310 respectively) than TC and finally OTC (table 5). The same behaviour was found by
311 Fernández-Calviño et al.,(2015) that reported higher desorption of OTC (12%) than TC
312 (8%) and CTC (7%).

313 The desorption percentage of OTC and TC was higher at pH 7 than pH 2 for the lowest
314 concentrations. However, desorption were always higher at pH 2 for the highest
315 concentrations. The different behavior in desorption depending on the pH can be
316 explained by the major ionic specie of the TCs at different pHs (Fig. 1). When the pH of
317 the solution is below 3.3 the TCs exist as cation, TCH_3^+ , due to the protonation of the
318 dimethylammonium group. A pH between 3.3 and 7.7 produces TCs species with
319 zwitterionic form TCH_2^\pm , due to the loss of a proton from the phenolic diketone fraction,
320 so the net charge of this species is zero (Chang et al., 2009b).

321 The hysteresis coefficient, H , for the sorption–desorption isotherms was calculated
322 according to $H = n_{\text{des}}/n_{\text{ads}}$ where n_{ads} and n_{des} are the Freundlich exponents obtained for
323 the sorption and desorption isotherms, respectively (Xu and Li, 2010). Usually, this
324 coefficient is attributed to the irreversible sorption of fractions of a chemical (Wan et
325 al., 2010). The hysteresis coefficients obtained in this study were higher than 0.8 for
326 CTC and OTC at pH 2 and 0.7 for TC. At pH 7, hysteresis coefficients were 0.3 for
327 OTC and TC, and 0.4 for CTC. Values of $H < 1$ indicated that the rate of desorption was
328 lower than sorption and the hysteresis took place for all the TCs. We concluded that
329 irreversible adsorption of a proportion of the tetracycline molecules was taking place in
330 the clay. Laird, (2007) found that different degrees of hysteresis were attributed to little
331 desorption and entrapment of adsorbed tetracycline within the matrix and irreversible
332 binding to specific adsorption sites.

333 **3.3.Adsorption mechanisms of TCs on stevensite**

334 IR spectroscopy was used as a technique to characterize IR active vibrations of the TCs
335 molecules and to clearly identify the interaction between TCs and the surface of the
336 adsorbent (Zhao et al., 2014). Fig. 5 showed the KMT-IR spectra of original
337 hydrochloride of OTC, TC and CTC and their respective spectra after adsorption on
338 stevensite. The most characteristic peaks of TCs are those in $1200\text{--}1700\text{ cm}^{-1}$ (Chang et
339 al., 2009b). Characteristic IR bands related with the functional groups of crystalline
340 OTC, TC and CTC hydrochlorides resulted peaks near $1675 - 1662\text{ cm}^{-1}$ for amide I
341 (the C=O group of the $-\text{CONH}_2$); 1640 cm^{-1} for amide II (N–H bonds of $-\text{CONH}_2$);
342 1616 and 1583 cm^{-1} for C=O groups of non-phenolic rings, 1525 and $1447\text{--}1458\text{ cm}^{-1}$
343 for skeletal C=C vibrations (aromatic ring), the band at 1410 cm^{-1} can be assigned to –
344 CH_3 deformation, the N-H of amino 1280 and 1267 cm^{-1} , and for C–N bonds 1228 cm^{-1}
345 (Chang et al., 2009a, 2009b, Zhao et al., 2015, 2012). The IR spectra of TCs adsorbed

346 on stevensite lacked peaks related with the C=O group of the amide and C-N bounds
347 therefore IR spectra demonstrated the role of amide and amine groups in the adsorption
348 of TCs on stevensite. In contrast, the two consecutive peaks at 1623 - 1580 cm^{-1} related
349 with C=O groups of non-phenolic rings and the peaks at 1525 and 1447 – 1458 cm^{-1} for
350 skeletal C=C vibrations (aromatic ring) appeared in the spectra of TCs adsorbed on
351 stevensite without displacement towards higher frequencies. Therefore the interaction
352 TCs – stevensite did not happened through these two functional groups. Too, the
353 presence of the two bands at 1525 and 1447 – 1458 cm^{-1} (C=O groups of non-phenolic
354 rings) suggests that the phenolic diketone group was protonated during the interaction
355 with stevensite (Chang et al., 2009a).

356 The most reported mechanism of TCs adsorption on clay minerals is cation exchange of
357 the positively charge of dimethyl-ammonium group of TCs and the negatively charged
358 clay minerals (Figuroa et al., 2004; Parolo et al., 2008; Zhao et al., 2015, 2012).

359 However this is not the unique mechanism, Zhao et al. (2012) described changes in
360 bands of amide carbonyl and amino groups and the carbonyl group in phenolic diketone
361 group in the FTIR spectra of TC equilibrated with montmorillonite. These changes
362 confirmed that TC was adsorbed into the clay via cation exchange and surface
363 complexation. Zhao et al. (2015) reported that TC adsorption on kaolinite and
364 montmorillonite mainly occurred at the dimethylamine group and, in the case of
365 kaolinite, the C=O of amide group over a wide pH range and, for both clays, at the
366 C=O group at non-phenolic ring under neutral to alkaline conditions but not under acid
367 conditions as happened in the present work. They purposed that the cation exchange of
368 the positively charged dimethylamine group in the TC molecule with the negatively
369 charged surface sites and the surface complexation of the C=O amide group and the
370 C=O group of phenolic diketone moiety with the variable charged edge sites are both

371 important mechanisms of TC adsorption onto kaolinite. (Wu et al., 2016) found that tri-
372 carbonil system of TC can strongly react with iron intercalated montmorillonite and also
373 form TC surface complexes. In summary, all of the authors previously cited
374 demonstrated that the main mechanism of TCs adsorption on different clays was the
375 cation exchange. In order to confirm this fact in TCs-stevensite system, an additional
376 interaction between stevensite and individual solutions of OTC, TC and CTC dissolved
377 in ultrapure water at initial concentration of 1000 mg L⁻¹ was performed per triplicate. A
378 control interaction with stevensite and ultrapure water was done in order to determine
379 the amount of Na, K, Ca and Mg dissolved in absence of TCs. The experimental
380 conditions were the same used in batch experiments described in section 2.2.
381 “Adsorption isotherms of TCs in stevensite and biochars”. After the interaction the
382 resulting concentrations of Na, K, Ca and Mg in solution were analyzed. Na and K were
383 determined by atomic emission spectrometry and Ca and Mg by atomic absorption
384 spectrometry (Perkin Elmer AA800). The results (table 6) showed significant increment
385 of Na, K, Ca and Mg concentrations after TCs adsorption on stevensite with respect to
386 control. The most important exchangeable cations were Mg and Ca. Therefore the TCs
387 adsorption mechanism on stevensite by cation exchange was confirmed.

388 Finally, in order to elucidate if TCs were adsorbed in the stevensite interlayers, an
389 aqueous suspension (25 mg L⁻¹) was prepared with 100 mg TC mg⁻¹ stevensite, near the
390 maximum adsorption values (table 5). It was smeared in a glass slide in order to obtain
391 an oriented aggregate for X-ray diffraction measurement of the basal spacing of the 2:1
392 sheet silicate smectitic material (i.e. Moore and Reynolds, 1997). In comparison to
393 natural stevensite (Fig. 5) with a basal spacing maximum measured at 15.0 Å (divalent
394 exchangeable cations), TC-stevensite showed an expanded basal spacing at 19.9Å, in
395 agreement with the expansion effect obtained by Aristilde et al. (2016, 2010). The

396 remaining 12.2 Å effect can be attributed to the existence of a small amount of the
397 monovalent Na-stevensite form as far as the batch experiments were conducted in a
398 NaNO₃ 0.01M aqueous medium. This data confirms the TC intercalation in the
399 interlayer space of the stevensite.

400

401 **3.4. Adsorption capacity of TCs in a continuous system.**

402 Stevensite was effective to adsorb TCs on continuous flow from artificial effluent which
403 composition was OTC, TC and CTC at 50 mg L⁻¹ in NaNO₃ 0.05 M at pH 7.0. Fig. 6
404 shows the relation between concentration of TCs at the entrance and at the exit of the
405 stevensite column. At high volume of polluted water passed through the system, the
406 relation nearly reached the value 1 which means that the system saturated.

407 The total adsorbed amount of TCs was 813 mg in 10 g of stevensite. This adsorption
408 corresponded to 34, 40 and 47% of total OTC, TC and CTC, respectively. The lower
409 adsorption comparing with adsorption isotherms was because the higher pH (7) and
410 ionic strength (0.05 M NaNO₃) of this solution and competitiveness between the three
411 TCs which were in the same solution and therefore they competed for the adsorption
412 sites of the stevensite. However, these new conditions were more realistic and similar to
413 wastewater than previous interactions. The lower saturation index of CTC than TC and
414 OTC (Fig.6) confirmed the highest affinity of stevensite for CTC and it agreed with
415 Langmuir and Freundlich models.

416 In the continuous system there was a total adsorption of 15.8 mg g⁻¹ for OTC, 26.6 mg
417 g⁻¹ for TC and 39.0 mg g⁻¹ for CTC at a total volume passed through the system of 10 L.
418 When comparing with their respective adsorption isotherms (table 5), the values of
419 Q_{max} were higher than 125 mg g⁻¹ for all the TCs concentrations . It was verified,

420 therefore, that the saturation of the material was not reached. As more mg of TCs were
421 adsorbed, more lost of adsorption capacity was observed, but the system did not never
422 become saturated. So the adsorption capacity of stevensite has been demonstrated in a
423 continuous flow.

424 Fig.7 shows the adsorption of TCs in the spiked wastewater effluent from the WWTP of
425 the Autonomous University of Madrid. The initial concentrations of TC, OTC and CTC
426 were 55, 42 and 37 mg L⁻¹ respectively, in spiked wastewater. After treatment by the
427 pressurized column filled with stevensite, the total adsorbed amount of TCs was 211 mg
428 in 10 g of stevensite. This means a total removal of 63, 75 and 75% for OTC, TC and
429 CTC, respectively. The saturation index (Fig.7) shows that the system is far away from
430 saturation (values lower than 0.4) and the clay affinity for TCs follows the sequence
431 CTC > TC > CTC.

432 The pH of the solution was around 7.5, so the TCs were in their zwitterionic form
433 TCH₂[±]. The zwitterions can be adsorbed on stevensite by cation exchange as was
434 described previously and by complexation with mineral cations (Aristilde et al., 2016b),
435 also increasing the negative charge on the surface of stevensite. At pH values higher
436 than 7 where hydroxyl groups (pKa 2) become increasingly negative, TCs can form
437 complexes with metal ions easily, thus adsorbing to stevensite (Yu - Jun et al., 2008).
438 Due to chelation generally reduces the bioavailability and therefore reduces the
439 antibacterial effect of the tetracyclines (Halling-Sorensen et al., 2002), the use of
440 stevensite clay in a continuous system for water remediation is viable.

441 Taking advantage of the affinity of the stevensite by the TCs, this adsorption (reached
442 more than the 60%) can be used in real wastewaters as an effective strategy to
443 decontaminate them.

444 **4. Conclusions**

445 Stevensite demonstrates higher potential to adsorb tetracyclines from water than
446 biochars. Stevensite shows great affinity for TCs, reaching maximum adsorption
447 capacity of 140 mg g⁻¹. The affinity of stevensite for TCs follows this preference: CTC
448 > TC > OTC. The ionic form of TCs adsorbed is the zwitterionic TCH_2^\pm at the pH range
449 assayed. Desorption phenomena is low with an appreciable hysteresis and the amount of
450 TC adsorbed on stevensite is more important than the pH of the solution for the
451 desorption process. The main mechanism of adsorption is cation exchange caused by
452 the interaction between the positive charge of the dimethyl-ammonium and the negative
453 surface of stevensite interlayer. However the amide group of TCs links also to
454 stevensite surface. In pressurized continuous system at laboratory scale, stevensite is
455 useful for TCs removal from wastewater.

456 For all of these reasons stevensite is an adequate adsorbent material to remove TCs
457 from wastewater and its implementation in WWTP is promising.

458 **5. Acknowledgements**

459 This work has been economically supported by Ministry of Economy and
460 Competitiveness of Spain (AGL2016-78490-R and CTM2013-47874-C2-2-R). CGD
461 was supported by a postdoctoral contract (Juan de la Cierva - Formación FJCI-2015-
462 23543) from the Spanish Ministry of Economy and Competitiveness.

463 **6. References**

464 Agency, E.M., 2013. Sales of veterinary antimicrobial agents in 26 EU / EEA countries
465 in 2013 Fifth ESVAC report.

466 Ahmed, M.B., Zhou, J.L., Ngo, H.H., Guo, W., 2015. Adsorptive removal of antibiotics
467 from water and wastewater: Progress and challenges. *Sci. Total Environ.* 532, 112–

468 126. doi:10.1016/j.scitotenv.2015.05.130

469 Akinbowale, O.L., Peng, H., Barton, M.D., 2016. Diversity of tetracycline resistance
470 genes in bacteria from aquaculture sources in Australia. *J. Appl. Microbiol.* 103,
471 2016–2025. doi:10.1111/j.1365-2672.2007.03445.x

472 Amin, M.F.M., Heijman, S.G.J., Rietveld, L.C., 2016. Clay – starch combination for
473 micropollutants removal from wastewater treatment plant effluent. *Water Sci.*
474 *Technol.* 73, 1719–1727. doi:10.2166/wst.2016.001

475 Andersen, S.R., Sandaa, R., 1994. Distribution of Tetracycline Resistance Determinants
476 among Gram-Negative Bacteria Isolated from Polluted and Unpolluted Marine
477 Sediments 60, 908–912.

478 Aristilde, L., Lanson, B., Miéché-brendlé, J., Marichal, C., Charlet, L., 2016a. Enhanced
479 interlayer trapping of a tetracycline antibiotic within montmorillonite layers in the
480 presence of Ca and Mg. *J. Colloid Interface Sci.* 464, 153–159.
481 doi:10.1016/j.jcis.2015.11.027

482 Aristilde, L., Lanson, B., Miéché-Brendlé, J., Marichal, C., Charlet, L., 2016b. Enhanced
483 interlayer trapping of a tetracycline antibiotic within montmorillonite layers in the
484 presence of Ca and Mg. *J. Colloid Interface Sci.* 464, 153–159.
485 doi:10.1016/j.jcis.2015.11.027

486 Aristilde, L., Marichal, C., Miéché-Brendlé, J., Lanson, B., Charlet, L., 2010.
487 Interactions of oxytetracycline with a smectite clay: A spectroscopic study with
488 molecular simulations. *Environ. Sci. Technol.* 44, 7839–7845.
489 doi:10.1021/es102136y

490 Bailey, L., Lekkerkerker, H.N.W., Maitland, G.C., 2014. Smectite clay - inorganic

491 nanoparticle mixed suspensions: phase behaviour and rheology. *Soft Matter* 11,
492 222–36. doi:10.1039/c4sm01717j

493 Berendonk, T.U., Manaia, C.M., Merlin, C., Fatta-Kassinos, D., Cytryn, E., Walsh, F.,
494 Bürgmann, H., Sørum, H., Norström, M., Pons, M.-N., Kreuzinger, N., Huovinen,
495 P., Stefani, S., Schwartz, T., Kisand, V., Baquero, F., Martinez, J.L., 2015.
496 Tackling antibiotic resistance: the environmental framework. *Nat. Rev. Microbiol.*
497 13, 310–317. doi:10.1038/nrmicro3439

498 Browne, J.E., Feldkamp, J.R., White, J.O.E.L., X, S.L.H.E.M., Lafayette, W., 1980.
499 Characterization and Adsorptive Properties of Pharmaceutical Grade Clays 69.

500 Chang, P.H., Li, Z., Jiang, W.-T., Kuo, C.-Y., Jean, J.-S., 2014. Adsorption of
501 tetracycline on montmorillonite: influence of solution pH, temperature, and ionic
502 strength. *Desalin. Water Treat.* 3994, 1–13. doi:10.1080/19443994.2014.924881

503 Chang, P.H., Li, Z., Jiang, W.T., Jean, J.S., 2009a. Adsorption and intercalation of
504 tetracycline by swelling clay minerals. *Appl. Clay Sci.* 46, 27–36.
505 doi:10.1016/j.clay.2009.07.002

506 Chang, P.H., Li, Z., Yu, T.L., Munkhbayer, S., Kuo, T.H., Hung, Y.C., Jean, J.S., Lin,
507 K.H., 2009b. Sorptive removal of tetracycline from water by palygorskite. *J.*
508 *Hazard. Mater.* 165, 148–155. doi:10.1016/j.jhazmat.2008.09.113

509 Cruz-Morató, C., Ferrando-Climent, L., Rodriguez-Mozaz, S., Barceló, D., Marco-
510 Urrea, E., Vicent, T., Sarrà, M., 2013. Degradation of pharmaceuticals in non-
511 sterile urban wastewater by *Trametes versicolor* in a fluidized bed bioreactor.
512 *Water Res.* 47, 5200–10. doi:10.1016/j.watres.2013.06.007

513 Ding, H., Wu, Y., Zou, B., Lou, Q., Zhang, W., Zhong, J., Lu, L., Dai, G., 2016.

514 Simultaneous removal and degradation characteristics of sulfonamide, tetracycline,
515 and quinolone antibiotics by laccase-mediated oxidation coupled with soil
516 adsorption. *J. Hazard. Mater.* 307, 350–358. doi:10.1016/j.jhazmat.2015.12.062

517 Fernández-calviño, D., Bermúdez-couso, A., Arias-estévez, M., Nóvoa-muñoz, J.C.,
518 Fernández-sanjurjo, M.J., Álvarez-rodríguez, E., Núñez-delgado, A., 2015.
519 Competitive adsorption / desorption of tetracycline , oxytetracycline and
520 chlortetracycline on two acid soils : Stirred flow chamber experiments.
521 *Chemosphere* 134, 361–366. doi:10.1016/j.chemosphere.2015.04.098

522 Figueroa, R.A., Leonard, A., Mackay, A.A., 2004. Modeling Tetracycline Antibiotic
523 Sorption to Clays. *Environ. Sci. Technol.* 38, 476–483. doi:10.1021/es0342087

524 Gavrilescu, M., Katerina, D., Aamand, J., Agathos, S., Fava, F., 2015. Emerging
525 pollutants in the environment: Present and future challenges in biomonitoring,
526 ecological risks and bioremediation. *N. Biotechnol.* 32, 147–156.
527 doi:10.1016/j.nbt.2014.01.001

528 González-Santamaría, D.E., López, E., Ruiz, A., Fernández, R., Ortega, A., Cuevas, J.,
529 2017. Adsorption of phenanthrene by stevensite and sepiolite. *Clay Minerals*
530 (accepted)

531 Halling-Sorensen, B., Sengelov, G., Tjornelund, J., 2002. Toxicity of tetracyclines and
532 tetracycline degradation products to environmentally relevant bacteria, including
533 selected tetracycline-resistant bacteria. *Arch. Environ. Contam. Toxicol.* 42, 263–
534 271. doi:10.1007/s00244-001-0017-2

535 Hou, J., Wang, C., Mao, D., Luo, Y., 2016. The occurrence and fate of tetracyclines in
536 two pharmaceutical wastewater treatment plants of Northern China. *Environ. Sci.*

537 Pollut. Res. 23, 1722–1731. doi:10.1007/s11356-015-5431-5

538 Jiang, W.T., Chang, P.H., Wang, Y.S., Tsai, Y., Jean, J.S., Li, Z., 2015. Sorption and
539 desorption of tetracycline on layered manganese dioxide birnessite. *Int. J. Environ.*
540 *Sci. Technol.* 12, 1695–1704. doi:10.1007/s13762-014-0547-6

541 Jing, X.R., Wang, Y.Y., Liu, W.J., Wang, Y.K., Jiang, H., 2014. Enhanced adsorption
542 performance of tetracycline in aqueous solutions by methanol-modified biochar.
543 *Chem. Eng. J.* 248, 168–174. doi:10.1016/j.cej.2014.03.006

544 Khoury, H.N., Eberl, D.D., Jones, B.F., 1982. Origin of magnesium clays from the
545 Amargosa Desert, Nevada. *Clays Clay Miner.* 30, 327–336.

546 Kim, S., Jensen, J.N., Aga, D.S., Weber, A.S., 2007. Tetracycline as a selector for
547 resistant bacteria in activated sludge 66, 1643–1651.
548 doi:10.1016/j.chemosphere.2006.07.066

549 Kühne, M., Ihnen, D., Möller, G., Agthe, O., 2000. Stability of Tetracycline in Water
550 and Liquid Manure. *Med. Vet.* 384, 379–384.

551 Kümmerer, K., 2009. Antibiotics in the aquatic environment – A review – Part II.
552 *Chemosphere* 75, 435–441. doi:10.1016/j.chemosphere.2008.12.006

553 Laird, D.A., 2007. Sorption of Tetracycline and Chlortetracycline on K- and Ca-
554 Saturated Soil Clays , Humic Substances , and Clay - Humic Complexes 41, 1928–
555 1933.

556 Liu, P., Liu, W., Jiang, H., Chen, J., Li, W., Yu, H., 2012a. Modification of bio-char
557 derived from fast pyrolysis of biomass and its application in removal of
558 tetracycline from aqueous solution. *Bioresour. Technol.* 121, 235–240.

559 doi:10.1016/j.biortech.2012.06.085

560 Liu, P., Liu, W.J., Jiang, H., Chen, J.J., Li, W.W., Yu, H.Q., 2012b. Modification of
561 bio-char derived from fast pyrolysis of biomass and its application in removal of
562 tetracycline from aqueous solution. *Bioresour. Technol.* 121, 235–240.
563 doi:10.1016/j.biortech.2012.06.085

564 Liu, S., Wu, P., Yu, L., Li, L., Gong, B., Zhu, N., Dang, Z., Yang, C., 2017. Preparation
565 and characterization of organo-vermiculite based on phosphatidylcholine and
566 adsorption of two typical antibiotics. *Appl. Clay Sci.* 137, 160–167.
567 doi:10.1016/j.clay.2016.12.002

568 López-Serna, R., Jurado, A., Vázquez-Suñé, E., Carrera, J., Petrović, M., Barceló, D.,
569 2013. Occurrence of 95 pharmaceuticals and transformation products in urban
570 groundwaters underlying the metropolis of Barcelona, Spain. *Environ. Pollut.* 174,
571 305–315. doi:10.1016/j.envpol.2012.11.022

572 Meffe, R., de Bustamante, I., 2014. Emerging organic contaminants in surface water
573 and groundwater: A first overview of the situation in Italy. *Sci. Total Environ.* 481,
574 280–295. doi:10.1016/j.scitotenv.2014.02.053

575 Meritxell, G., Petrovic, M., Barceló, D., 2007. Wastewater treatment plants as a
576 pathway for aquatic contamination by pharmaceuticals in the Ebro river basin
577 (northeast Spain). *Environ. Chem.* 26, 1553–1562.

578 Mohd Amin, M.F., Heijman, S.G.J., Rietveld, L.C., 2016. Clay-starch combination for
579 micropollutants removal from wastewater treatment plant effluent. *Water Sci.*
580 *Technol.* 73, 1719–1727. doi:10.2166/wst.2016.001

581 Moore, D.M., Reynolds, R.C., 1997. X-Ray Diffraction and the Identification and

582 Analysis of Clay Minerals, 2nd ed. Oxford University Press, New York.

583 Osorio, V., Pérez, S., Ginebreda, A., 2012. Pharmaceuticals on a sewage impacted
584 section of a Mediterranean River (Llobregat River, NE Spain) and their
585 relationship with hydrological conditions. *Environ. Sci. Pollut. Res.* 19, 1013–
586 1025. doi:10.1007/s11356-011-0603-4

587 Pal, R., Megharaj, M., Kirkbride, K.P., Naidu, R., 2013. Illicit drugs and the
588 environment - A review. *Sci. Total Environ.* 463–464, 1079–1092.
589 doi:10.1016/j.scitotenv.2012.05.086

590 Parolo, M.E., Savini, M.C., Vallés, J.M., Baschini, M.T., Avena, M.J., 2008.
591 Tetracycline adsorption on montmorillonite: pH and ionic strength effects. *Appl.*
592 *Clay Sci.* 40, 179–186. doi:10.1016/j.clay.2007.08.003

593 Qambrani, N.A., Rahman, M.M., Won, S., Shim, S., Ra, C., 2017. Biochar properties
594 and eco-friendly applications for climate change mitigation, waste management,
595 and wastewater treatment: A review. *Renew. Sustain. Energy Rev.* 79, 255–273.
596 doi:10.1016/j.rser.2017.05.057

597 Srinivasan, P., Sarmah, A.K., Smernik, R., Das, O., Farid, M., Gao, W., 2015. A
598 feasibility study of agricultural and sewage biomass as biochar, bioenergy and
599 biocomposite feedstock: Production, characterization and potential applications.
600 *Sci. Total Environ.* 512–513, 495–505. doi:10.1016/j.scitotenv.2015.01.068

601 Tan, X., Liu, Y., Zeng, G., Wang, X., Hu, X., Gu, Y., 2015. Chemosphere Application
602 of biochar for the removal of pollutants from aqueous solutions. *Chemosphere.*
603 doi:10.1016/j.chemosphere.2014.12.058

604 Valcárcel, Y., Alonso, S.G., Rodríguez-Gil, J.L., Romo-Maroto, R., Gil, A., Catalá, M.,

605 2011. Analysis of the presence of cardiovascular and analgesic/anti-
606 inflammatory/antipyretic pharmaceuticals in river- and drinking-water of the
607 Madrid Region in Spain. *Chemosphere* 82, 1062–71.
608 doi:10.1016/j.chemosphere.2010.10.041

609 Wan, Y., Bao, Y., Zhou, Q., 2010. *Chemosphere* Simultaneous adsorption and
610 desorption of cadmium and tetracycline on cinnamon soil. *Chemosphere* 80, 807–
611 812. doi:10.1016/j.chemosphere.2010.04.066

612 Wu, H., Xie, H., He, G., Guan, Y., Zhang, Y., 2016. Effects of the pH and anions on the
613 adsorption of tetracycline on iron-montmorillonite. *Appl. Clay Sci.* 119, 161–169.
614 doi:10.1016/j.clay.2015.08.001

615 Xu, X.-R., Li, X.-Y., 2010. Sorption and desorption of antibiotic tetracycline on marine
616 sediments. *Chemosphere* 78, 430–6. doi:10.1016/j.chemosphere.2009.10.045

617 Yao, F., Zhaojun, L., Xiaoqing, H., 2016. Impacts of soil organic matter , iron-
618 aluminium oxides and pH on adsorption-desorption behaviors of oxytetracycline
619 Impacts of soil organic matter , iron-aluminium oxides and pH on adsorption-
620 desorption behaviors of oxytetracycline. *Res. J. Biotechnol.* 11, 121–131.

621 Yao, Y., Gao, B., Inyang, M., Zimmerman, A.R., Cao, X., Pullammanappallil, P., Yang,
622 L., 2011. *Bioresource Technology* Biochar derived from anaerobically digested
623 sugar beet tailings : Characterization and phosphate removal potential. *Bioresour.*
624 *Technol.* 102, 6273–6278. doi:10.1016/j.biortech.2011.03.006

625 Yu - Jun, W., De - A n, J., R ui - Juan, S., H ao - Wen, Z., Dong - Mei, Z., 2008.
626 Adsorption and Cosorption of Tetracycline and Copper (II) on Montmorillonite as
627 Affected by Solution pH. *Environ. Sci. Technol* 42, 3254–3259.

- 628 Zhao, Y., Gu, X., Gao, S., Geng, J., Wang, X., 2012. Adsorption of tetracycline (TC)
629 onto montmorillonite: Cations and humic acid effects. *Geoderma* 183–184, 12–18.
630 doi:10.1016/j.geoderma.2012.03.004
- 631 Zhao, Y., Gu, X., LI, S., Han, R., Wang, G., 2015. Insights into tetracycline adsorption
632 onto kaolinite and montmorillonite: experiments and modeling. *Environ. Sci.*
633 *Pollut. Res.* 22, 17031–17040. doi:10.1007/s11356-015-4839-2
- 634 Zhao, Y., Tong, F., Gu, X., Gu, C., Wang, X., Zhang, Y., 2014. Insights into
635 tetracycline adsorption onto goethite: Experiments and modeling. *Sci. Total*
636 *Environ.* 470–471, 19–25. doi:10.1016/j.scitotenv.2013.09.059
- 637

638 **Figure captions**

639 Fig. 1. Chemical structure of oxytetracycline (OTC), tetracycline (TC) and
640 chlortetracycline (CTC) and their corresponding acid dissociation constants (pK_a) (Ding
641 et al., 2016).

642 Fig. 2. Adsorption isotherms of TCs in stevensite (A), biochar of holm oak (B) and
643 biochar from mixture of pruning (C). Bars indicate standard deviation ($n=3$).

644 Fig 3. Percentage of adsorbed CTC, TC and OTC on stevensite after adsorption
645 isotherm (Ads Initial) and after successive desorption isotherm at pH 2 (remain pH 2)
646 and pH 7 (remain pH 7). Bars represent standard deviation ($n=3$).

647 Fig. 4. IR spectra of oxitetracycline hydrochloride (OTC), tetracycline hydrochloride
648 (TC) and (CTC) chlortetracycline hydrochloride and OTC, TC and CTC adsorbed on
649 stevensite.

650 Fig. 5: XRD diffraction patterns of TC treated stevensite (red) and natural stevensite
651 (black), measured with a $CuK\alpha$ anode using a X'PERT PANalytical instrument with an
652 X-CELERATOR detector. Peaks are marked in Å using the Bragg equation: d -spacing
653 $= (\lambda(CuK\alpha (1.54 \text{ \AA}))/2\text{Sen}(\Theta))$. $2\theta(\Theta)$ is the detector position angle related to the X-
654 ray incident angle. 10 \AA peak corresponds to illite impurities.

655 Fig.6. Breakthrough curves for spiked water with tetracyclines (OTC, TC and CTC) on
656 stevensite.

657 Fig.7. Breakthrough curves for spiked wastewater with tetracyclines (OTC, TC and
658 CTC) on stevensite.

Table 1: Compilation of adsorption experiments with tetracyclines on different materials.

Material	TCs adsorbed (mg g⁻¹)	pH	References
Kaolinite	47	5	(Zhao et al., 2011)
Montmorillonite	250	5.5	(Zhao et al., 2012)
	>300	3	
Montmorillonite	287	4	(Parolo et al., 2008)
	133	7	
Na-Montmorillonite	>300		
Ca- Montmorillonite	> 300	4.5	(Chang et al., 2009)
Vermiculite	36.8	-	(Liu et al., 2017)
Organo-vermiculite	66.4	-	(Liu et al., 2017)
Active carbon	>300	7	(Acosta et al., 2016)
Mono-layer carbon nanotubes	>300		
Multi-layer carbon nanotubes	44	3	(Ji and Chen, 2009)
Active carbon	9		
Graphite	3		
Marine sediments	31	7.5	(Xu and Li, 2010)
Iron	24	3	(Hanay et al., 2014)

Table 2: Properties of Minclear N100 Clay (Mohd Amin et al., 2016; González-Santamaría et al., 2017).

Mineralogy	Trade mark	Composition	BET area (m ² g ⁻¹)	CIC (cmol c Kg ⁻¹)	pH	Apparent Density (mg cm ⁻³)
Smectite	Minclear N100	stevensite (>90 %), illite (<5%) dolomite (<5 %), feldspar and quartz impurities (<1%)	221 ± 2	60-70	8.6	500 - 600

Table 3: Basic physico-chemical characterization of holm oak biochar (HO) and biochar from mixture of pruning (M).

Biochar	pH	EC ($\mu\text{S}\cdot\text{cm}^{-1}$)	Organic Matter (%)	BET area ($\text{m}^2\text{ g}^{-1}$)	Granulometry (mm)	Pyrolysis temperature ($^{\circ}\text{C}$)
HO	9.29 ± 0.03	494 ± 17	79.6 ± 0.4	76.4 ± 1.4	< 8	500
M	9.73 ± 0.03	944 ± 25	89.6 ± 0.1	30.4 ± 0.4	< 2 (50% < 0.5)	900

Table 4: Linear gradient elution program of tetracyclines analysis by HPLC.

Time (min)	Flow (mL min⁻¹)	TFA 10mM (%)	Acetonitrile (%)	Methanol (%)
0	1.5	95	4	1
7.5	1.5	70	24	6
13.5	1.5	65	28	7
15	1.5	95	4	1

TFA: trifluoroacetic acid solution in water

Table 5: Freundlich and Langmuir adsorption coefficients of oxytetracycline (OTC), tetracycline (TC) and chlortetracycline (CTC) in stevensite, biochar of holm oak (OH) and biochar from mixture of pruning (M).

		Freundlich			Langmuir		
		K	n	R ²	a _L	Q _{max}	R ²
Stevensite	OTC	29.13	3.79	0.992	0.052	126.1	0.988
	TC	40.19	4.65	0.987	0.112	127.1	0.986
	CTC	54.03	5.05	0.980	0.291	139.9	0.975
Biochar OH	OTC	0.776	1.82	0.976	0.002	44.22	0.976
	TC	4.902	7.24	0.792	0.071	11.85	0.914
	CTC	1.922	2.86	0.863	0.014	17.64	0.768
Biochar M	OTC	1.948	2.80	0.946	0.007	24.57	0.988
	TC	3.755	4.98	0.901	0.015	15.15	0.980
	CTC	6.076	4.92	0.994	0.168	18.48	0.923

Table 6: Concentration (mean \pm standard deviation, $n = 3$) of water soluble cations from stevensite (control) and concentration of desorbed cations after tetracyclines (OTC: oxytetracycline; TC tetracycline and CTC: chlortetracycline) adsorption on stevensite. Asterisks denotes significant differences between control and samples ($p < 0.05$).

	Control	OTC	TC	CTC
	mg L⁻¹			
Na	1.48 \pm 0.01	1.83* \pm 0.15	1.84* \pm 0.06	1.73* \pm 0.05
K	1.58 \pm 0.05	1.96* \pm 0.04	1.81* \pm 0.05	1.80* \pm 0.04
Ca	< 0.045	8.56* \pm 0.50	10.4* \pm 1.69	2.12* \pm 0.26
Mg	7.13 \pm 1.24	17.6* \pm 0.22	17.7* \pm 0.33	17.9* \pm 0.09

Figure 1

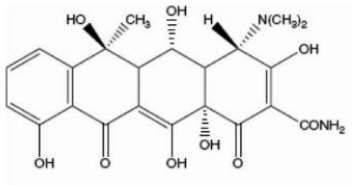
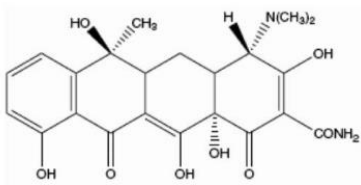
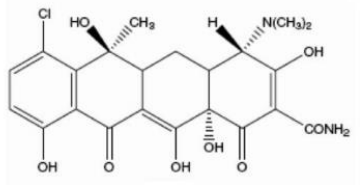
	Oxytetracycline (OTC)	Tetracycline (TC)	Chlortetracycline (CTC)
			
pK_a1	3.3	3.3	3.3
pK_a2	7.3	7.7	7.4
pK_a3	9.1	9.7	9.3

Figure 2

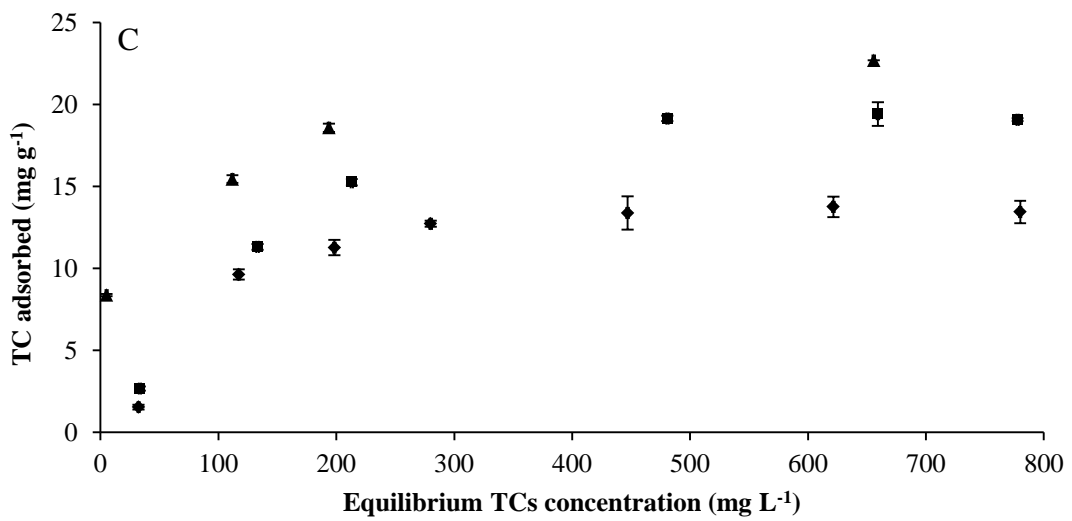
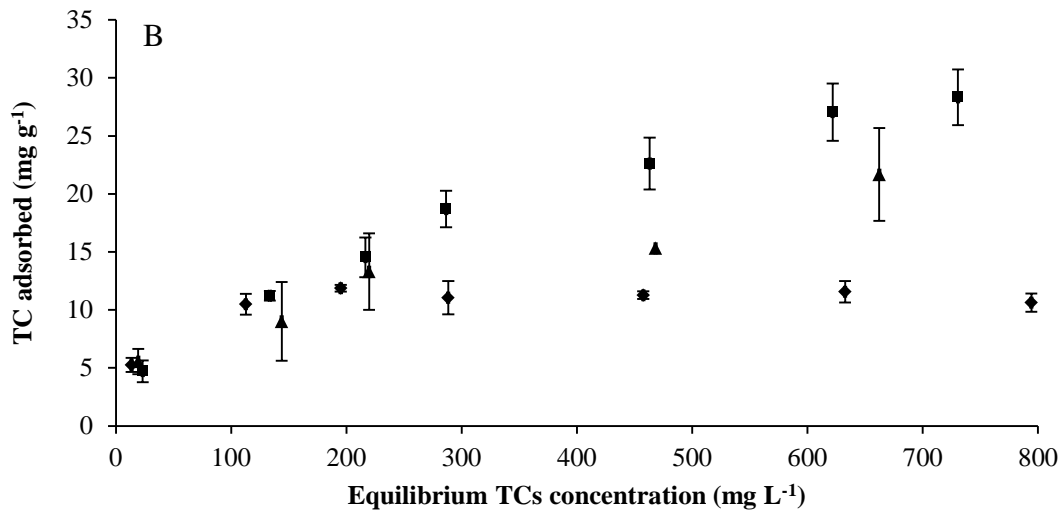
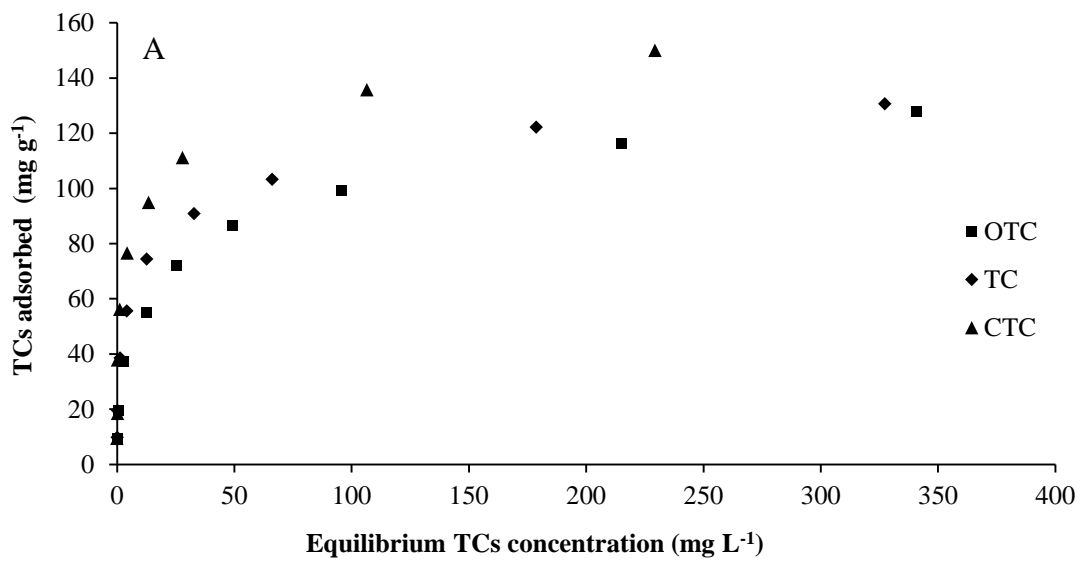


Figure 3

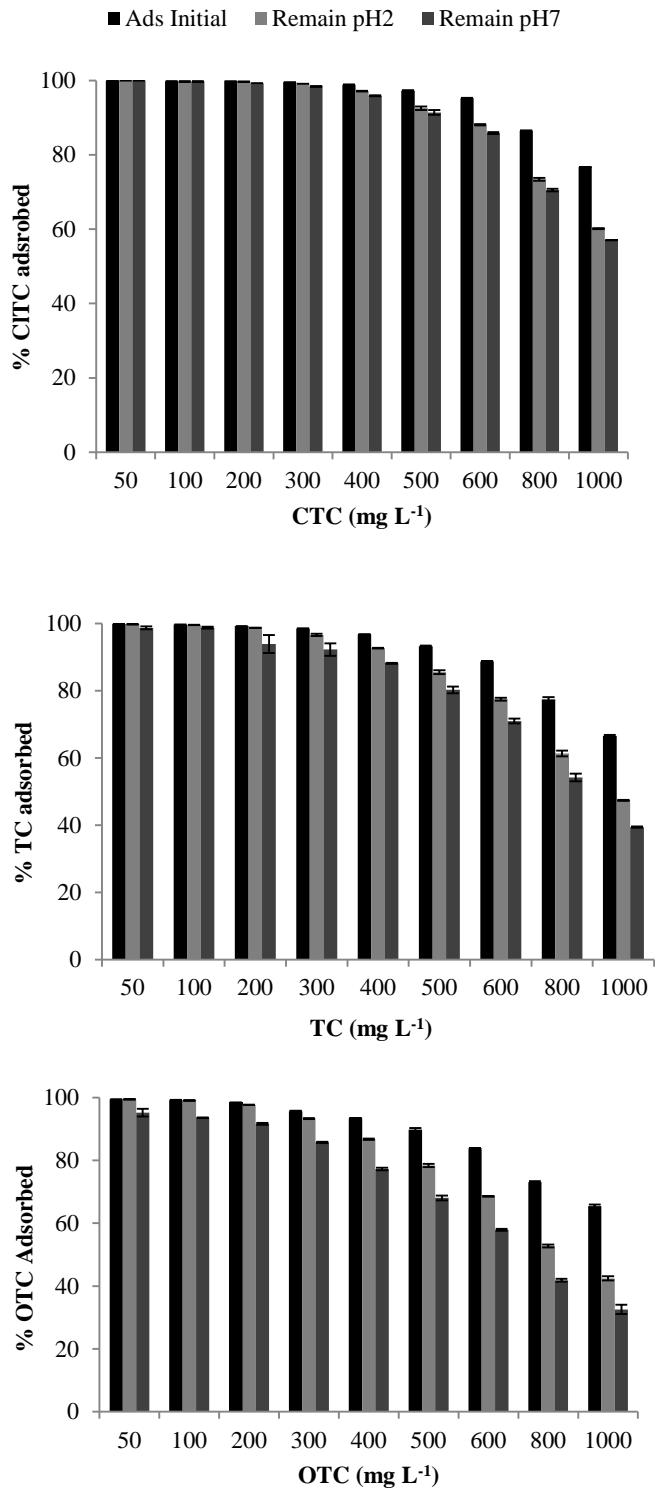


Figure 4

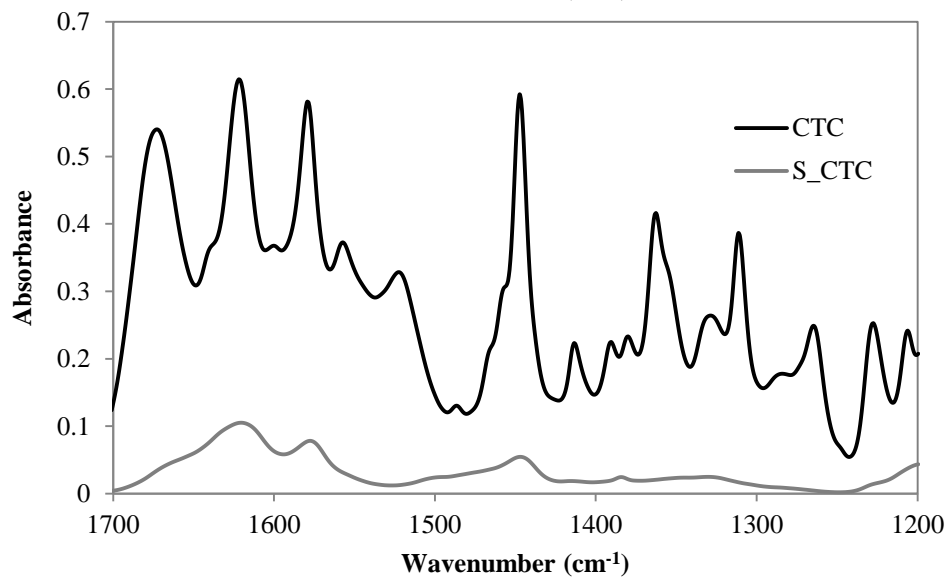
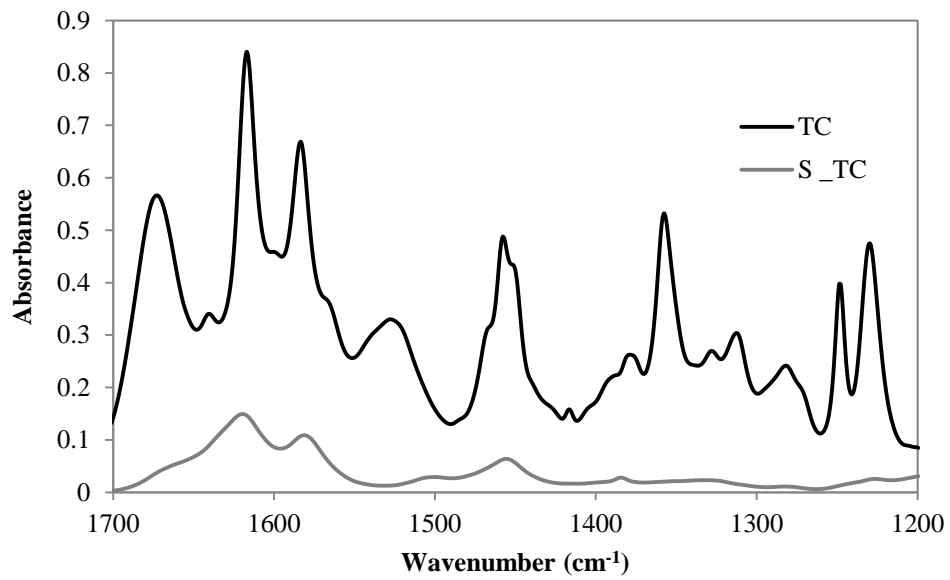
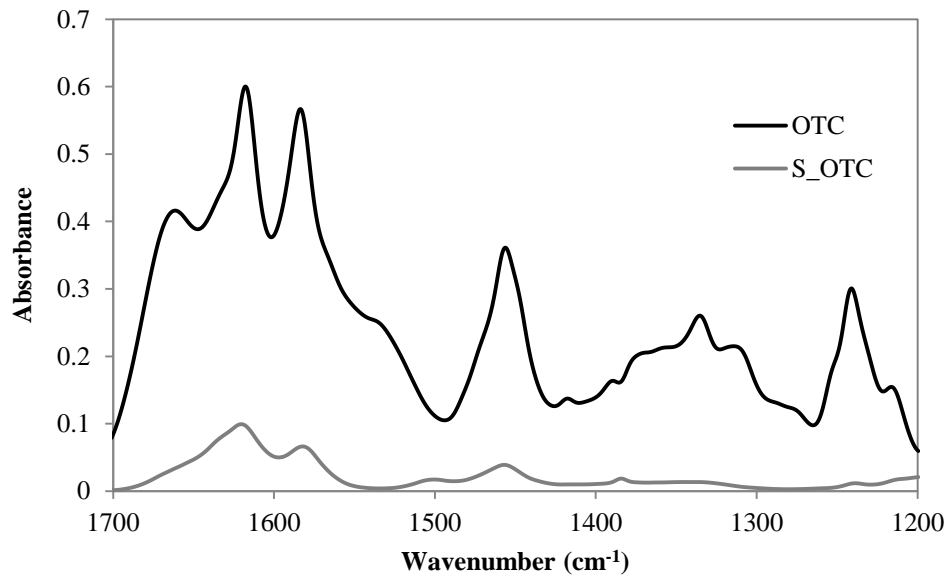


Figure 5

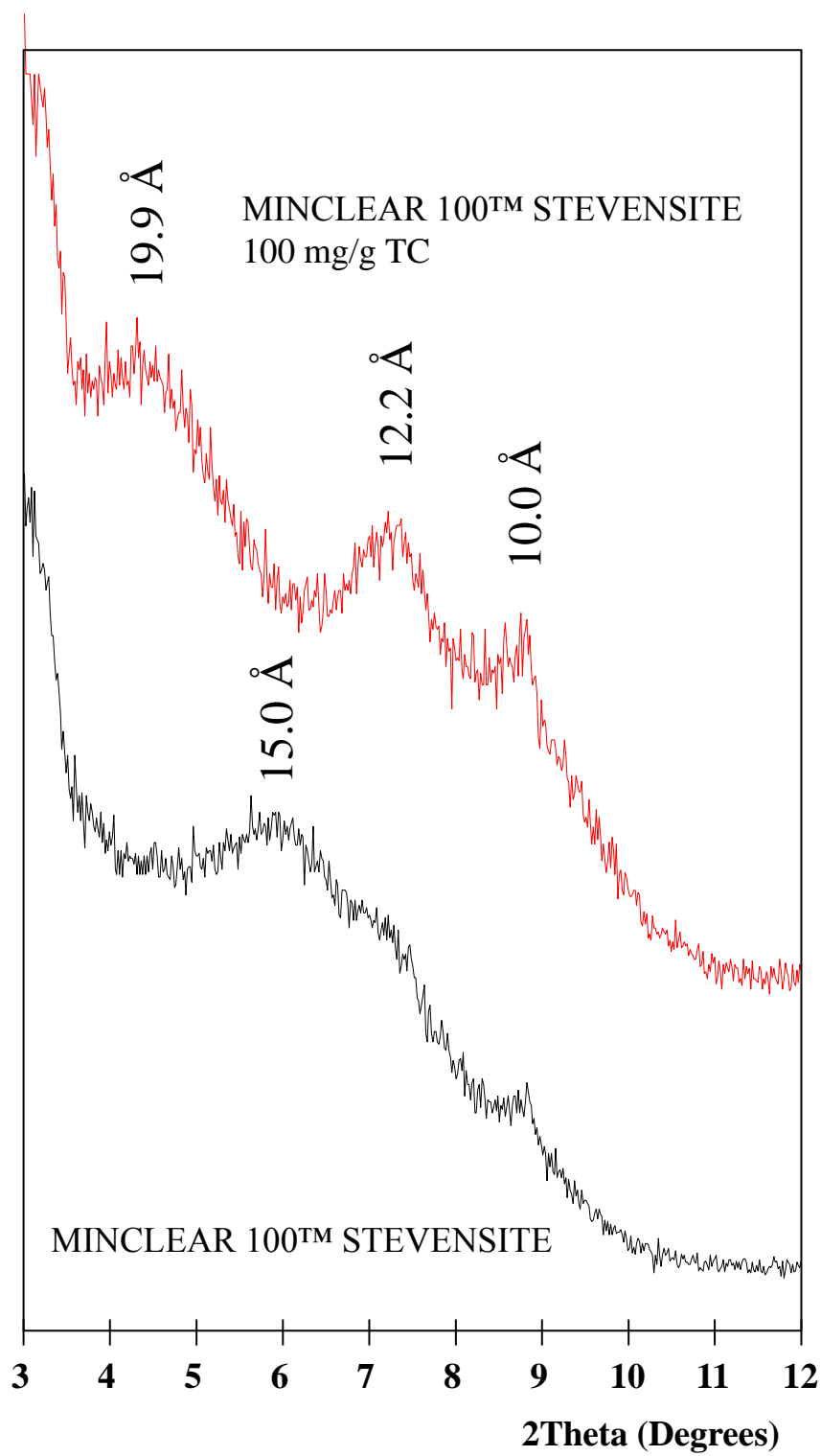


Figure 6

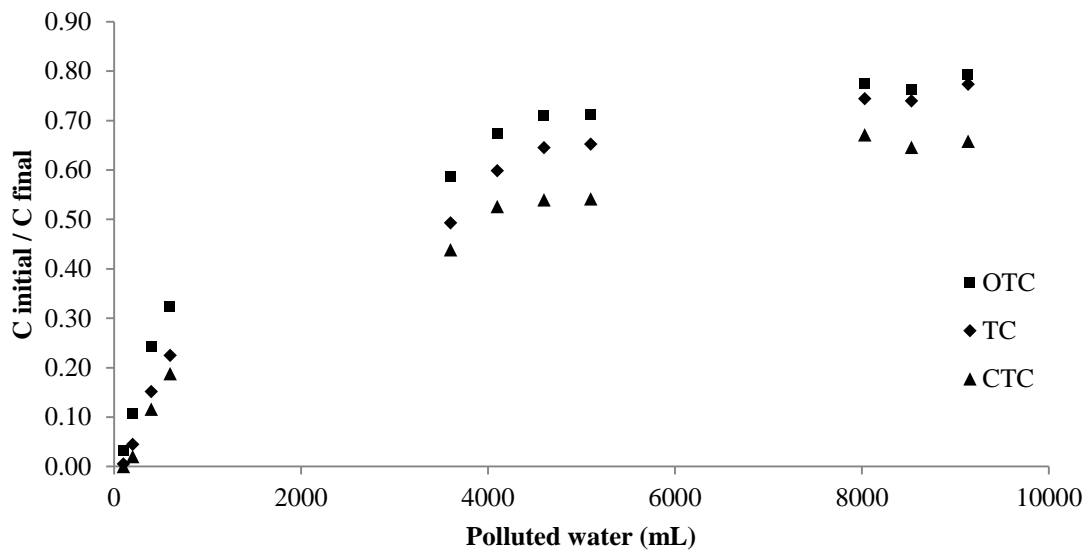


Figure 7

